

# The synchrotron component study in a spectral energy distribution of blazars

M. G. Mingaliev,<sup>1,2</sup> Yu. V. Sotnikova,<sup>1</sup> T. V. Mufakharov,<sup>1</sup> A. K. Erkenov,<sup>1</sup> and R. Yu. Udovitskiy<sup>1</sup>

<sup>1</sup>*Special Astrophysical Observatory of RAS, Nizhnij Arkhyz, 369167 Russia*

<sup>2</sup>*Kazan Federal University, 18 Kremlyovskaya St., Kazan, 420008, Russia\**

We study the synchrotron component of the spectral energy distribution (SED) on the sample of 877 blazars using the ASDC SED Builder Tool with available broadband data from the literature. Our sample includes 423 flat-spectrum radio sources (FSRQs), 361 BL Lac objects and candidates, and 93 blazars of uncertain type. We have made an estimation of the synchrotron peak frequency ( $\nu_{peak}^s$ ) for the 875 objects and further classified them as high, intermediate and low synchrotron peaked sources (HSPs/ISPs/LSPs). There are 42 HSPs with  $\nu_{peak}^s > 10^{16.5}$  Hz, 222 ISPs with  $10^{14.5} < \nu_{peak}^s < 10^{16.5}$  Hz, and 611 LSPs with  $\nu_{peak}^s < 10^{14.5}$  Hz in our sample. We have calculated an average value of  $\nu_{peak}^s$  to be  $10^{13.4 \pm 1.0}$  Hz for FSRQs and  $10^{14.6 \pm 1.4}$  Hz for BL Lacs. We found out that  $\nu_{peak}^s$  and the flux density at 4.8 GHz have a different distribution (as indicated by Kolmogorov–Smirnov test at significance level 0.05) for the FSRQ and BL Lac blazars, and for the RBL and XBL types of BL Lacs. Distribution of  $\nu_{peak}^s$  values is broader for BL Lacs, than for FSRQs. There are no ultra-high energy peaked objects (with  $\nu_{peak}^s > 10^{19}$  Hz) in our BL Lac sample according to our estimations. The significant part of FSRQs (41%) and small part of BL Lacs (9%) in our sample could be considered as candidates to the very-low synchrotron peaked blazars (with  $\nu_{peak}^s < 10^{13}$  Hz). Our foundations confirm results of the previous studies made on samples with significantly smaller number of objects.

Keywords: quasars: general—BL Lacertae objects: general—galaxies: nuclei—galaxies: jets— radio continuum: galaxies

*Will appear in Astrophysical Bulletin, Volume 70, Issue 3, pp.264-272, 2015*

## 1. INTRODUCTION

The blazars are active galactic nuclei (AGNs) with the jet, viewed at small angles to the observer [1]. This characteristic feature explains various observational properties of this class of objects. Due to strong magnetic fields in the jet, non-thermal radiation dominates over the entire range of the electromagnetic spectrum of blazars. Blazars are historically divided into two subclasses: flat-spectrum radio quasars (FSRQs) and BL Lacertae type objects (BL Lacs). The optical spectrum of FSRQs reveals strong broad emission lines, while the spectrum of BL Lac objects often have no lines, sometimes possessing weak emission or absorption lines. Blazars are characterized by variable non-thermal radiation in all frequency bands. The spectral energy distribution (SED) of blazars has two characteristic components: a low frequency component with a peak in the optical, ultraviolet, or X-ray spectral region and a high frequency component with a peak in the gamma-ray band. Their presence is usually explained by synchrotron radiation and the effect of inverse Compton scattering [2]. Most of the blazar radiation from the radio to optical band (and in some cases, in X-rays) is the synchrotron radiation of charged particles in the jet (see, e.g., [3–6]).

In addition to the division of blazars into the FSRQ and BL Lac types by the presence or absence of lines in the optical spectrum, there is also a classification of blazars by the synchrotron peak frequency ( $\nu_{peak}^s$ ) in their SED. Blazars divided into high/intermediate/low-synchrotron peaked, according to the  $\nu_{peak}^s$ : high synchrotron peaked (HSPs) ones with the  $\nu_{peak}^s > 10^{16.5}$  Hz, low synchrotron peaked (LSPs) blazars with the  $\nu_{peak}^s < 10^{14.5}$  Hz, and intermediate synchrotron-peaked (ISPs) have  $10^{14.5} < \nu_{peak}^s < 10^{16.5}$  Hz. In this paper we use this classification, proposed by Urry and Padovani [1].

The BL Lac blazars are traditionally divided into RBLs (radio-selected), OBLs (optical-selected) and XBLs (X-ray-selected) depending on the band in which they were originally identified: radio, optical, or X-rays [7–13]. Typically, they differ in the position of the synchrotron component on the SED. For the RBLs, the synchrotron component peak more often falls into the radio to IR frequency range, for the XBL-objects it resides in the UV-X-ray band [14]. Such a historical division of BL Lac objects into XBLs and RBLs is often not related to the physical differences of the objects themselves [1]. Some BL Lacs that were not detected

---

\* E-mail:marat@sao.ru

in the X-rays are regarded as XBL blazars due to the high X-ray/radio flux ratio [15, 16]. For example, PKS 0548–32, PKS 2005–48 and PKS 2155–30, or optically identified Mrk 180, Mrk 421 and Mrk 501 are considered as XBL-type [17].

The shape of the SEDs of the blazars and the  $\nu_{peak}^s$  value may change depending on the activity of the object, sometimes significantly, by orders of magnitude [18, 19]. In those cases object could be considered as a “transition” type, within the simplified model in which the blazar type and its radio luminosity are determined by the degree of activity of a given radio galaxy (FRI and FRII) [20, 21].

Nieppola, Tornikoski, and Valtaoja [22] determined  $\nu_{peak}^s$  for about 300 BL Lacs using the literature data. Subsequently, researchers of broadband properties of blazars referred to this study, even though the literature data it used was non-homogeneous (except for the radio band data). Over the recent years, the number of blazars with available observed data has greatly increased. At the same time, there appeared new measurements for the objects from this sample, defining the position of  $\nu_{peak}^s$ . In this study, we list the ultra-high-energy synchrotron-peak (UHBLs) BL Lac candidates, with  $\nu_{peak}^s > 10^{19}$  Hz. For half of them, according to our estimates,  $\nu_{peak}^s$  values appeared to be significantly smaller, although still almost all of these objects can be referred to as HSP ( $\nu_{peak}^s > 10^{16.5}$  Hz). In [23] the same group of researchers determined  $\nu_{peak}^s$  for 135 blazars.

Giommi et al. [24] have obtained broadband SEDs for 105 bright blazars ( $F_{radio} > 1$  Jy) and calculated  $\nu_{peak}^s$  based on the simultaneous observations of the Planck, Swift, and Fermi telescopes. As a result, an average  $\nu_{peak}^s$  of  $\nu_{peak}^s = 10^{13.1 \pm 0.1}$  Hz was determined for FSRQs. For BL Lac blazars, this value is higher, and the distribution of  $\nu_{peak}^s$  is broader. The results of that work are well consistent with [25], where empirical relations were derived to determine  $\nu_{peak}^s$  from the broadband spectral indices (radio-optical and optical-X-ray) for 48 bright blazars from the Fermi list. The values  $\log \nu_{peak}^s \sim 13$  and  $\log \nu_{peak}^s \sim 15$  were found for FSRQ and BL Lac blazars respectively. In the second AGN catalogue of the Fermi telescope (2LAC), an analytical formula similar to [25] was used for finding  $\nu_{peak}^s$ , and for most of the FSRQs  $\nu_{peak}^s < 10^{14}$  Hz was obtained, while for the BL Lac objects it was  $\nu_{peak}^s > 10^{15}$  Hz [26].

Meyer et al. [27] have measured  $\nu_{peak}^s$  for a relatively large sample of 216 blazars.

Determination of the synchrotron peak frequency ( $\nu_{peak}^s$ ), and the blazar type along with it, is an important task for researchers of the AGN phenomenon, as this parameter affects the distribution of radiating particles by the energies in the jet, as well as physical processes and the state of the matter in the emission region. Making the measurements of  $\nu_{peak}^s$  based on observations of a large number of blazars, one can test other empirical relationships which are used to compute this parameter in the lack of experimental data.

The aim of this work is to study the synchrotron component of the spectral energy distribution of a sample of 877 blazars. The objects are systematically observed with the RATAN-600 radio telescope. 361 sources of our sample are the BL Lac objects and candidates, representing 25% of all known blazars of this type<sup>1</sup>, 423 are the FSRQ-type blazars, and 93 are the blazars of uncertain type.

## 2. THE SAMPLE AND OBSERVATIONS

We have studied 877 blazars from the RATAN-600 monitoring list, objects are presented in Table 1. The full version of Table 1 is available at the Strasbourg astronomical Data Center (CDS)<sup>2</sup>. Notes for the columns in Table 1: (1) NVSS name, (2) alias, (3) redshift  $z$ , (4) R-band magnitude (USNO), (5) the logarithm of the synchrotron peak frequency obtained in the present work, (6) correlation coefficient between the experimental data and the theoretical curve used in the calculations of  $\nu_{peak}^s$ , (7) flux density at a frequency of 4.8 GHz and its standard error, obtained with the RATAN-600, (8) blazar type based on the position of the synchrotron component on the SED: LSP ISP HSP, (9) blazar type according to the classification of [28], (10) BL Lac type, based on the band in which it was originally identified: RBL — radio-selected BL Lac, XBL — X-ray-selected BL Lac.

The redshifts of the objects are taken from the Roma-BZCAT catalogue<sup>3</sup> [28] or from the NED. The Roma-BZCAT is the most popular catalogue of the blazars, based on a large number of various surveys with

---

<sup>1</sup> according to the Roma-BZCAT, 5th edition

<sup>2</sup> <http://vizier.cfa.harvard.edu/>

<sup>3</sup> <http://www.asdc.asi.it/bzcat/>

**Table 1.** List of the studied blazars

NVSS name	Alias	$z$	$R_{mag}$	$\log \nu_{peak}^s$ [Hz]	$k$	$F_{4.8GHz} \pm \sigma$ , Jy	SED class	Blazar type	Selection type
000520+052411	BZQJ0005+0524	1.900	16.2	15.17	0.90	$0.126 \pm 0.004$	ISP	FSRQ	-
000557+382015	GB6B0003+3803	0.229	17.6	13.28	0.92	$0.470 \pm 0.019$	LSP	FSRQ	-
000613-062335	PKS0003-066	0.347	17.9	12.93	0.95	$2.118 \pm 0.049$	LSP	BL Lac	RBL
000649+242236	CGRaBSJ0006+2422	1.684	18.8	14.27	0.91	$0.132 \pm 0.012$	LSP	FSRQ	-
000759+471207	BZBJ0007+4712	0.280	18.2	13.66	0.86	$0.064 \pm 0.005$	LSP	BL Lac	RBL
001031+105830	PGC737	0.089	15.8	13.92	0.94	$0.120 \pm 0.005$	LSP	FSRQ	-
001101-261233	PKS0008-264	1.096	18.8	13.97	0.91	$0.600 \pm 0.024$	LSP	FSRQ	-
001354-042352	PKS0011-046	1.075	19.7	12.58	0.92	$0.230 \pm 0.009$	LSP	FSRQ	-

**Table 2.** Sample subpopulation classes

Designation criterion	Class	Number
Optical spectrum	BL Lac	296
	BL Lac cand.	65
	Blazar un.type	93
	FSRQ	423
Selection method	RBL	327
	XBL	124
	OBL	3
SED type	LSP	611
	ISP	222
	HSP	42

the use of observed data from different wavelength ranges. The average redshift for the FSRQs is  $z = 1.446$ , and for the BL Lac and candidates it is  $z = 0.443$ .

Table 2 shows the distribution of objects by their types. For the classification of blazars by the optical spectrum, we used the Roma-BZCAT: FSRQ — flat-spectrum radio quasar, BL Lac — BL Lacertae type object, BL Lac.cand. — BL Lacertae candidate, Blazar un.type — blazar of uncertain type.

We have made the division of BL Lac blazars (a total of 454, including the candidates and blazars of uncertain type) by the type of their detection (RBL, XBL, or OBL) from literature data (see the references in the BLcat catalogue<sup>4</sup> [29]). The classification of blazars by the SED type was done in this work by the criteria set out in [1].

The flux density distribution for the sources of the sample at a frequency of 4.8 GHz is shown in Fig. 1. The subsample of FSRQs consists of the brightest objects at the radio band: the average flux density at a frequency of 4.8 GHz (according to the RATAN-600 data) for them is 0.736 Jy. The subsample of BL Lac blazars is formed from the sources that are weaker in the radio band with an average  $F_{4.8GHz} = 0.355$  Jy. Table 3 lists the average values of some parameters of the objects of our sample.

Most of the measurements of BL Lac objects are available in the on-line BLcat catalogue. Some measurements of FSRQs presented in this paper contain new RATAN-600 observations carried out with two radiometric complexes in 2014–2015. Parameters of the antenna and the receiving systems of RATAN-600 secondary mirrors №1 and №2 are presented in Table 4 (the secondary mirrors are marked as “1” and “2” respectively). The columns contain: (1) central frequency in GHz, (2) bandwidth in GHz, (3) detection limit by the flux density per angular resolution unit (mJy/beam), (4) angular resolution at the right ascension (arcsec) at the intermediate antenna incidence angles ( $\delta \sim 42^\circ$ ).

The technique of observations and calibration of measurements are described, for example, in [29, 30].

<sup>4</sup> <http://www.sao.ru/blcat/>

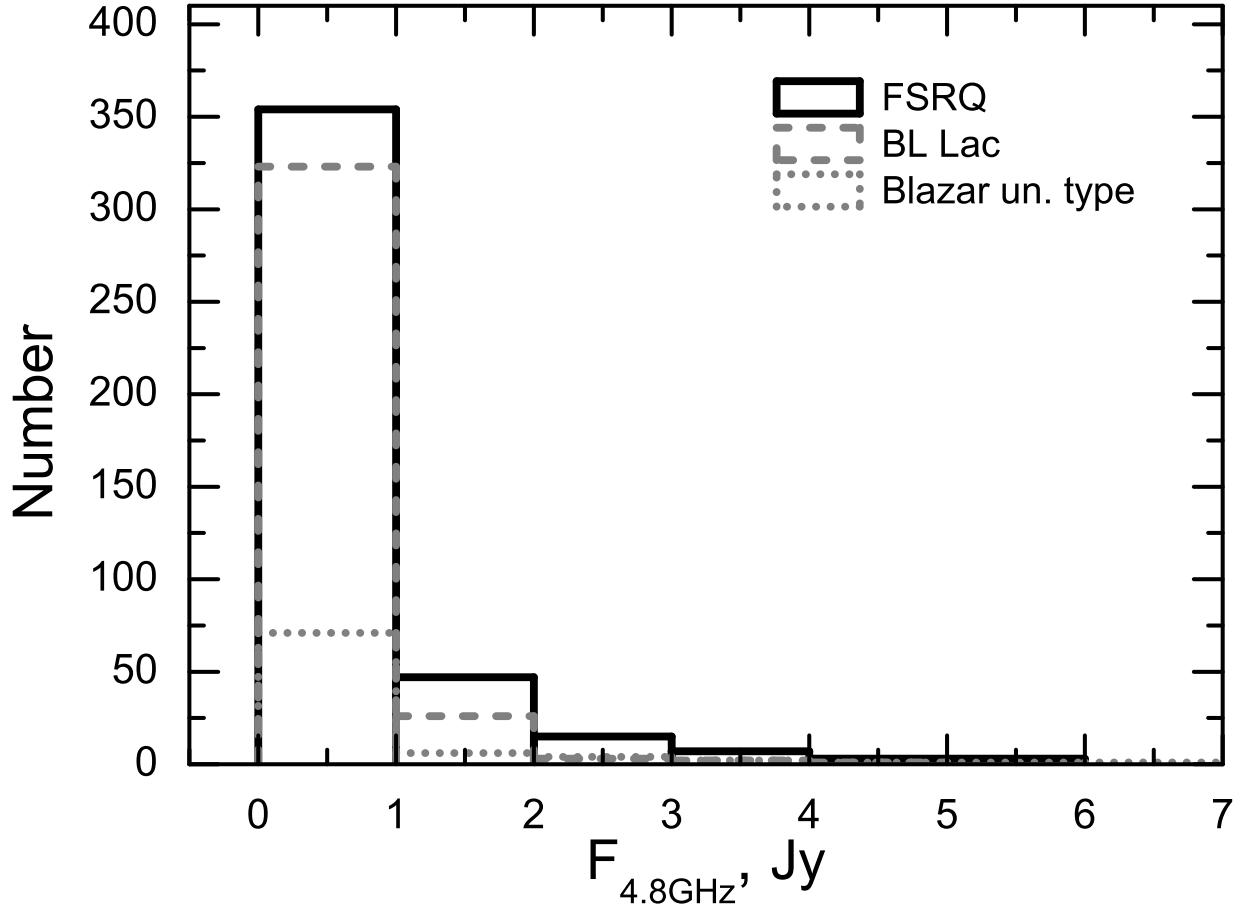


**Figure 1.** The flux density distribution for the sources of the sample at 4.8 GHz, measured with the RATAN-600. Three objects (PKS B1226+023, PKS 1253-055 и PKS 1921-293) with the  $F_{4.8GHz} > 6$  Jy were excluded from distribution for clarity of the display

**Table 3.** The average values of some parameters for different subclasses of blazars (the number of measurements is shown in the lower index)

Blazar type	$z$	$\log \nu_{peak}$ [Hz]	$F_{4.8GHz}$ , Jy	$R_{mag}$
FSRQ	1.446 <sub>422</sub>	$13.4 \pm 1.0$ <sub>422</sub>	0.736 <sub>423</sub>	18.6 <sub>423</sub>
BL Lac	0.443 <sub>253</sub>	$14.6 \pm 1.4$ <sub>360</sub>	0.355 <sub>359</sub>	17.3 <sub>358</sub>
Blazar un.type	0.499 <sub>86</sub>	$13.9 \pm 1.1$ <sub>93</sub>	0.739 <sub>93</sub>	17.2 <sub>92</sub>
RBL	0.53 <sub>234</sub>	$13.9 \pm 0.9$ <sub>326</sub>	0.624 <sub>329</sub>	14.3 <sub>325</sub>
XBL	0.30 <sub>102</sub>	$15.9 \pm 1.3$ <sub>124</sub>	0.089 <sub>123</sub>	16.7 <sub>123</sub>

### 3. THE SYNCHROTRON PEAK FREQUENCY ESTIMATION

The SEDs were constructed in the  $\log \nu - \log \nu F_\nu$  plane. The synchrotron component can be described by a polynomial of the second or third degree:

$$\log(\nu F_\nu) = A(\log \nu)^2 + B(\log \nu) + C$$

$$\log(\nu F_\nu) = A(\log \nu)^3 + B(\log \nu)^2 + C(\log \nu) + D,$$

where A, B, C and D are the coefficients. Hence:

$$\log \nu_{peak} = -B/2A.$$

**Table 4.** Some parameters of the RATAN-600 antenna and continuum radiometers

$f_0$ , GHz		$\Delta f_0$ , GHz		$\Delta F$ , mJy/beam		$\theta_{RA}$ , arcsec
1	2	1	2	1	2	
21.7	21.7	2.5	2.5	70	88	11
11.2	11.2	1.4	1.0	20	20	16
7.7	-	1.0	-	25	-	22
4.8	4.8	0.9	0.8	8	11	36
2.3	-	0.4	-	30	-	80
1.1	-	0.12	-	160	-	170

Column description: (1) – central frequency , (2) – bandwidth, (3) – flux density detection limit per beam, (4) – angular resolution (at RA).

**Figure 2.** The SED of the PKS 0017+200, visualised with the ASDC SED Builder Tool

We used the ASDC SED Builder Tool<sup>5</sup> [31] to calculate the synchrotron peak frequency. It allows building broadband SEDs of sources and approximate the experimental data by a theoretical curve. The system is based on the local catalogues covering a wide range of the electromagnetic spectrum, from radio to gamma-

<sup>5</sup> <http://tools.asdc.asi.it>

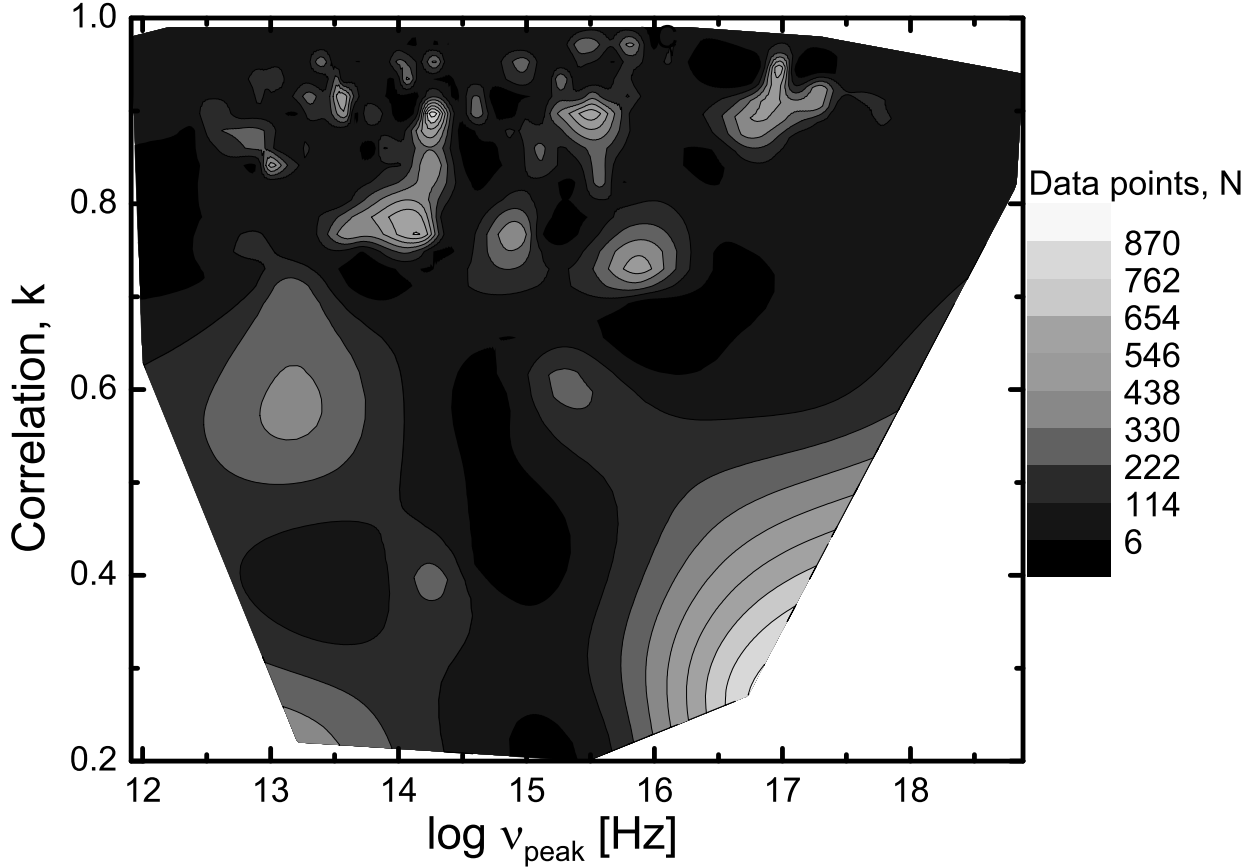


**Figure 3.** The  $\nu_{peak}^s$ —correlation coefficient—measurements number relation for BL Lacs

rays.

In the present study we used the polynomial of the second or third degree. The correlation coefficient is given in the sixth column of Table 1. The example of the approximation for the PKS 0017+200 given in Fig. 2.

Determination of the synchrotron peak frequency often depends on the data set and calculation method, because of the inhomogeneity of the experimental data. If there is a lot of measurements at one band but only a few points at the other bands, even overall measurements number is big, there will be a weak correlation between experimental data points and theoretical curve, and, therefore, uncertain estimation of the  $\nu_{peak}^s$  parameter.

Fig. 3 gives an example of the relationship between the calculated value of  $\nu_{peak}^s$ , the correlation coefficient, and the number of measurements for BL Lac blazars of the sample. The colours show the number of measurements  $N$  used for construction of the SED curve for each object: white corresponds to the maximum number of measurements ( $N = 870$ ), and black means the minimum ( $N = 6$ ). It is clearly seen that a low correlation of the theoretical curve and the experimental data is observed both for a small and a large number of measurements (700–900 points). This is related not only with inhomogeneity of measurements at certain frequencies but also with object variability, as a result of which a large scatter of data is observed when non-simultaneous measurements are used. And conversely, at a small number of measurements (up to one hundred), high correlation can be observed, when several points are easily described by any polynomial.

Fig. 3 also demonstrates that the region of  $10^{17} < \nu_{peak}^s < 10^{19}$  Hz differs by a small number of measurements (in most cases up to one hundred). Therefore, the  $\nu_{peak}^s$  values obtained for the HSP blazars can be refined and calculated more reliably with the increasing number of measurements at these frequencies.

An overestimation of  $\nu_{peak}^s$  is possible when taking into account thermal radiation in the optical/UV bands; in some objects this thermal component makes a significant contribution [20]. The deficiency of observational data in the X-rays, on the contrary, leads to an underestimation of  $\nu_{peak}^s$ .

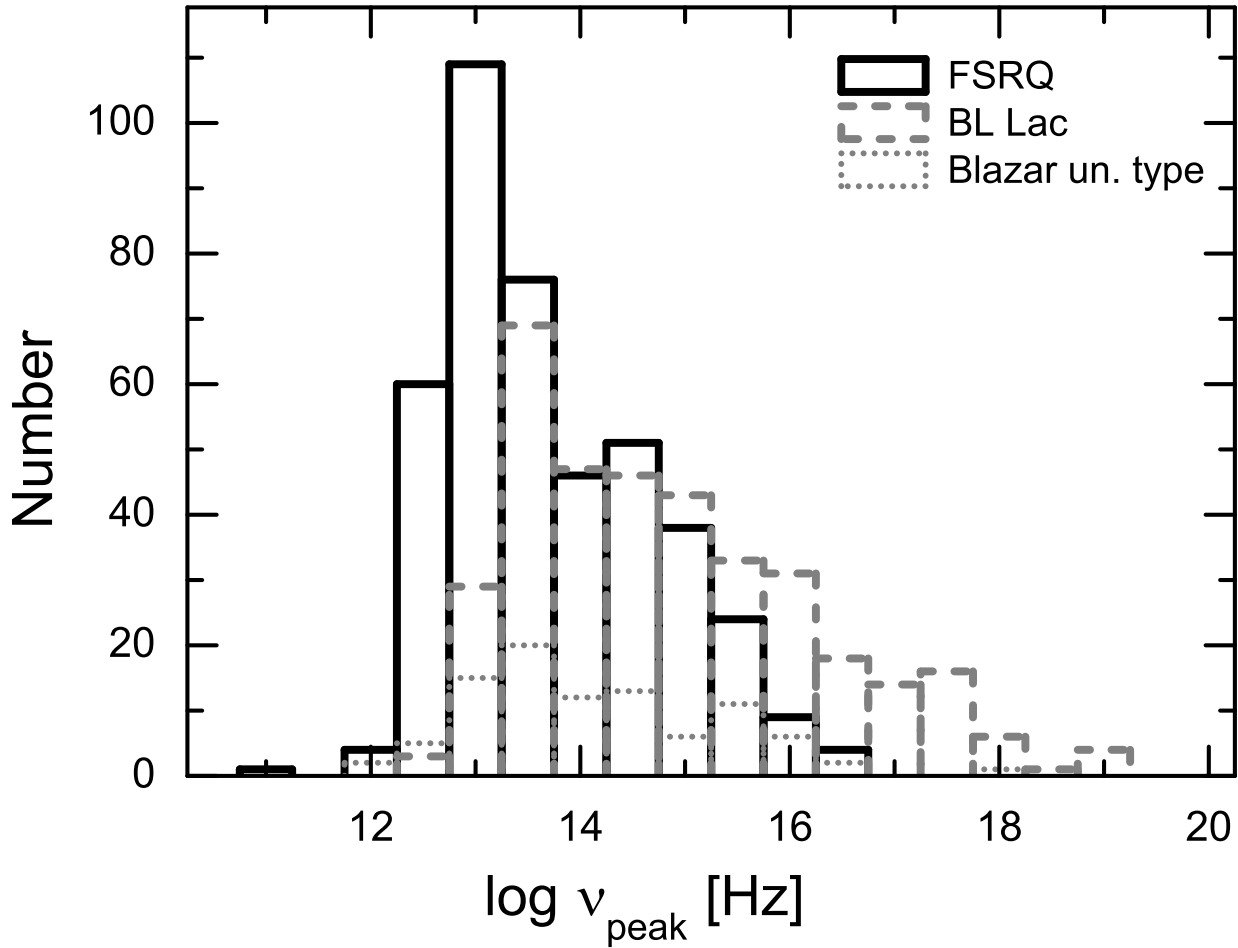


Figure 4. Distribution of  $\nu_{peak}^s$  for FSRQs, BL Lacs and blazars of uncertain type

## 4. RESULTS

### 4.1. The $\nu_{peak}^s$ values

The calculations of  $\nu_{peak}^s$  were made in the observers frame. The  $\nu_{peak}^s$  have been obtained for 875 blazars of the sample and are presented in the fifth column of Table 1. We could not estimate  $\nu_{peak}^s$  for two objects TEX 0537+251 and BZQ J1102+5941 because lack of measurements at frequencies exceeding  $10^{15}$  Hz. The distribution of  $\nu_{peak}^s$  for FSRQs and BL Lacs is presented in Fig. 4.

The average values of the  $z$ ,  $\log \nu_{peak}^s$ ,  $F_{4.8GHz}$  and  $R_{mag}$  are given in Table 3.

The  $\nu_{peak}^s$  and  $F_{4.8 GHz}$  samples for FSRQs, BL Lacs and RBLs, XBLs are drawn from different distributions, according to the Kolmogorov-Smirnov (K-S) test (at the 0.05 significance level).

The  $\nu_{peak}^s - F_{4.8GHz}$  relations for the FSRQs and BL Lacs are shown in Fig. 5. The flux density of blazars obtained with the RATAN-600 at a frequency of 4.8 GHz is presented in Table 1 (column 7). The distribution of  $\nu_{peak}^s$  for the BL Lac objects and candidates is wider, with an average of  $10^{14.6 \pm 1.4}$  Hz ( $10^{11.9} - 10^{18.9}$  Hz). The distribution of  $\nu_{peak}^s$  for the FSRQs has an average value of  $10^{13.4 \pm 1.0}$  Hz, and most of the values are located in the range from  $10^{11.9}$  to  $10^{16.5}$  Hz.

### 4.2. RBL and XBL objects

The classification of BL Lac objects to the RBL and XBL types was made using literature data and is presented in Table 1 (column 10). The sample consist of 327 RBLs, 124 XBLs and 3 OBLs. The

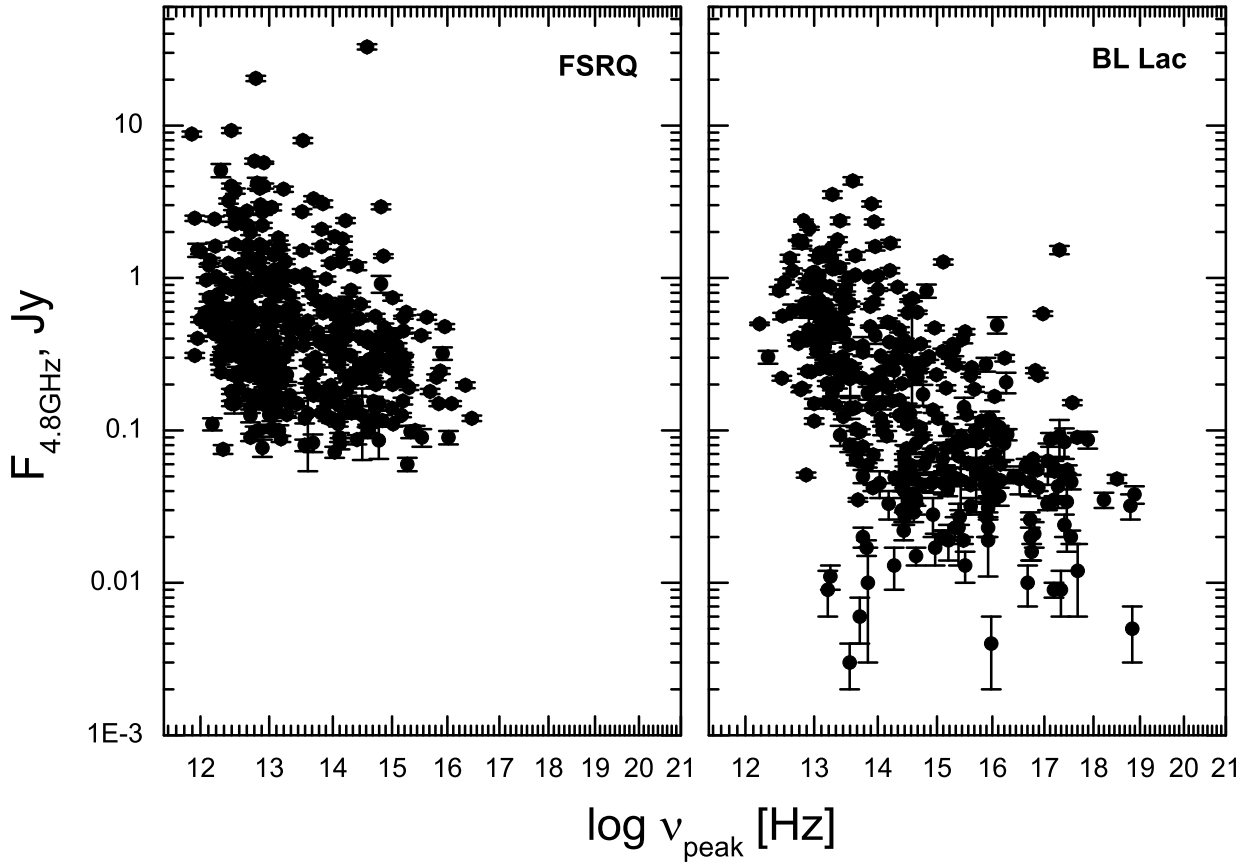


**Figure 5.** The  $\nu_{peak}^s$ –flux density at 4.8 GHz ( $F_{4.8GHz}$ ) relation for FSRQs and BL Lacs. The mean value of  $\nu_{peak}^s$  is  $10^{13.4 \pm 1.0}$  Hz for FSRQs and  $10^{14.6 \pm 1.4}$  Hz for BL Lacs and candidates

$\nu_{peak}^s - F_{4.8GHz}$  relations for the RBL and XBL objects are shown in Fig. 6. On average,  $\nu_{peak}^s$  values for the RBLs is less than that for the XBLs. The average  $\nu_{peak}^s$  for the RBLs is  $10^{13.9 \pm 0.9}$  Hz, and for the XBLs it is  $10^{15.9 \pm 1.3}$  Hz.

The distribution of peak frequencies for the XBLs is broader ( $10^{13.2} - 10^{18.9}$  Hz) than for the RBLs ( $10^{11.9} - 10^{16.3}$  Hz). The average flux densities  $F_{4.8GHz}$  for the XBLs and RBLs differ significantly (see Table 3).

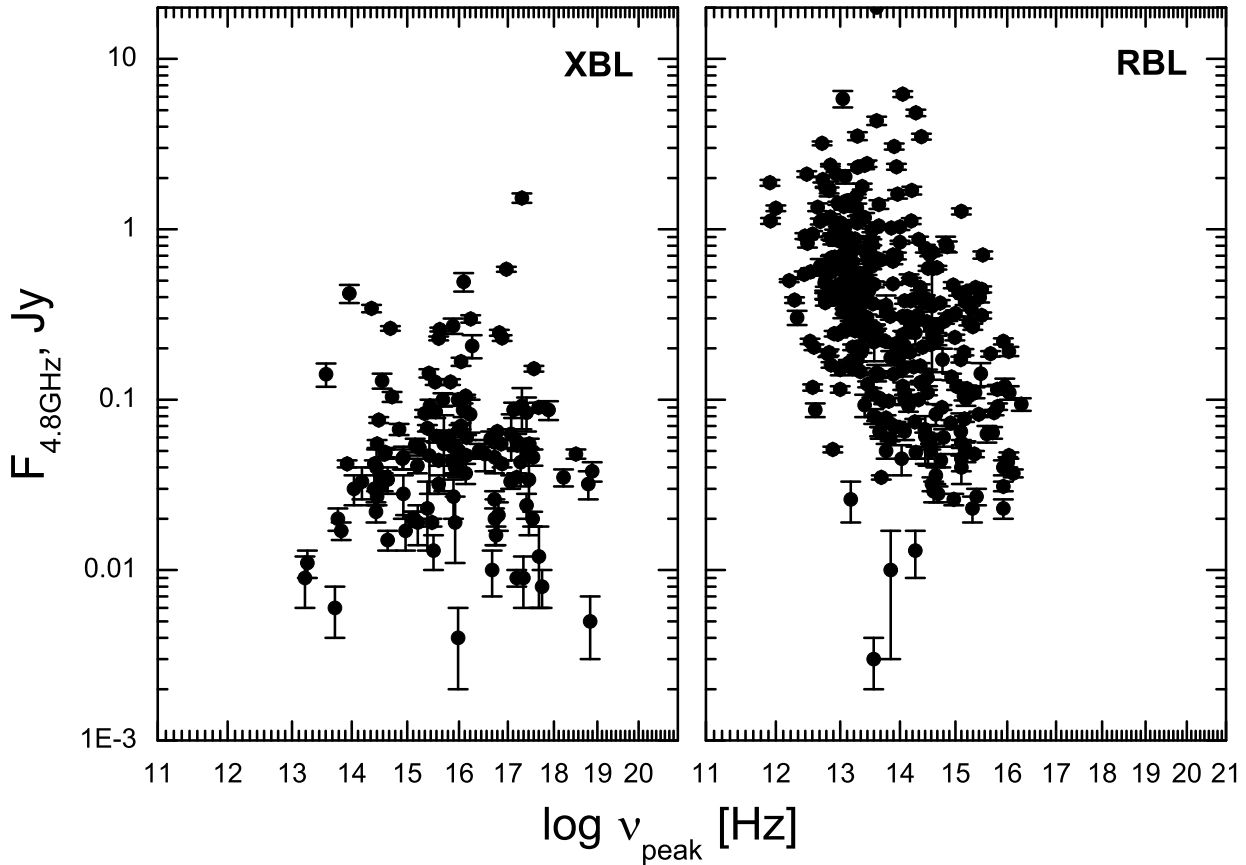
#### 4.3. UHBL candidates

Table 5 gives a list of blazars which were considered in [22] as UHBL candidates (ultra-high energy-peaked BL Lac objects). The blazars with a synchrotron component peak frequency of  $\nu_{peak}^s > 10^{19}$  Hz were related to this class of objects. The first column gives the name of an object. The second and third columns of Table 5 represent the measurements of  $\log \nu_{peak}^s$  in [22] and in the present work, respectively. The fourth column lists the flux density at a frequency of 4.8 GHz and its error, obtained with the RATAN-600. The fifth column contains the amplitude of object variability (in percent) at a frequency of 4.8 GHz and the number of measurements, which are indicated at the lower index, according to the RATAN-600 data. The amplitude variability was determined by the formula:

$$Var_F = \frac{(F_i - \sigma_i)_{max} - (F_i + \sigma_i)_{min}}{(F_i - \sigma_i)_{max} + (F_i + \sigma_i)_{min}},$$

where  $F_{max}$  and  $F_{min}$  are the maximum and minimum flux density,  $\sigma_{F_{max}}$  and  $\sigma_{F_{min}}$  are their errors. The sixth column presents the type of a BL Lac by the identification band, taken from the literature. No UHBL candidates were found in our sample according to this classification. The maximum value of  $\nu_{peak}^s$  in this sample is measured for the objects 1ES 0229+200 ( $10^{18.5}$  Hz), 1ES 0502+675 ( $10^{18.9}$  Hz) and





**Figure 6.** The  $\nu_{peak}^s - F_{4.8GHz}$  relation for RBL and XBL objects. The mean value of  $\nu_{peak}^s$  is  $10^{13.9 \pm 0.9}$  and  $10^{15.9 \pm 1.3}$  Hz for RBLs and XBLs, respectively

RXJ1458.4+4832 ( $10^{18.8}$  Hz). All objects listed in Table 5 are belong to the XBL subclass of BL Lac objects. The UHBL candidates list is composed of the objects faint in the radio domain, with the flux densities not exceeding 100 mJy at a frequency of 4.8 GHz (column 4 of Table 5). Almost all the objects are variable in the radio band: the amplitude of variability ranges from a few to tens of percent. Some of them were observed insufficiently, only 3–5 times. In other frequency ranges they have also been scarcely measured. Being historically discovered in X-rays, they were hence probably mostly observed in this very spectral region and thus became UHBL candidates.

#### 4.4. VLSP candidates

Along with the high/low-synchrotron peaked blazars, there is so-called very low synchrotron peaked blazars (VLSP,  $\nu_{peak}^s < 10^{13}$  Hz) were recently denoted [32, 33]. The maximum of the synchrotron component in them falls into the IR/mm spectral region.

Ghisellini et al. [34] described the relationship between the maximum energy of electrons  $\gamma_{peak}$  and the density of the total energy ( $U_{ph} + U_B$ ), where  $U_{ph}$  is the density of photon energy, and  $U_B$  is the energy density of the magnetic field in the jet:

$$\gamma_{peak} \sim (U_{ph} + U_B)^{-0.6}.$$

If we assume that the total energy density is  $U = L/R^2$ , where  $L$  is the luminosity of the jet and  $R$  is its size, and that the synchrotron peak frequency  $\nu_{peak}^s \propto \gamma_{peak}^2$ , then objects of high luminosity have a lower peak frequency. Hence, objects with a very low value of  $\nu_{peak}^s$  would often be quite bright radio sources. In fact, most of the objects in our sample of VLSP candidates are the FSRQs (41% of the total number of FSRQs) and only 9% are the BL Lacs.

**Table 5.** UHBL candidates ( $\log \nu_{peak}^s > 19$ ) from [22]. The  $\log \nu_{peak}^s$  values are presented for 2006 in column 2 (from [22]) and for 2015 in column 3 (results of this work, signed RATAN). The flux density and variability index values, measured at 4.8 GHz with the RATAN-600, are shown in the columns (4) and (5)

Name	$\log \nu_{peak}^s$ , [22]	$\log \nu_{peak}^s$ , RATAN	$F_{4.8GHz}$ , Jy	$\text{Var } F_{4.8Nobs}$ , %	Selected type
1ES 0229+200	19.45	18.50	$0.049 \pm 0.003$	7.5 <sub>5</sub>	XBL
RXS J0314.3+0620	19.57	16.13	$0.038 \pm 0.005$	1.5 <sub>5</sub>	XBL
2E 0323+0214	19.87	15.92	$0.041 \pm 0.003$	17.1 <sub>7</sub>	XBL
2E 0414+0057	20.71	16.78	$0.065 \pm 0.002$	22.0 <sub>7</sub>	XBL
1ES 0502+675	19.18	18.88	$0.038 \pm 0.005$	18.4 <sub>6</sub>	XBL
EXO 0706.1+5913	21.05	17.88	$0.087 \pm 0.011$	1.8 <sub>6</sub>	XBL
RXS J0847.2+1133	19.13	17.40	$0.024 \pm 0.004$	-	XBL
1ES 0927+500	21.13	17.40	$0.084 \pm 0.019$	56.6 <sub>5</sub>	XBL
RXS J1008.1+4705	19.67	17.33	$0.009 \pm 0.003$	76.5 <sub>3</sub>	XBL
RXS J1012.7+4229	20.97	17.46	$0.055 \pm 0.004$	13.8 <sub>8</sub>	XBL
EXO 1149.9+2455	19.83	16.72	$0.026 \pm 0.003$	12.2 <sub>3</sub>	XBL
PG 1218+304	19.14	16.86	$0.055 \pm 0.003$	8.3 <sub>5</sub>	XBL
RXS J1319.5+1405	19.67	15.15	$0.055 \pm 0.005$	12.4 <sub>5</sub>	XBL
RXS J1341.0+3959	20.97	14.59	$0.048 \pm 0.003$	8.2 <sub>6</sub>	XBL
RXS J1353.4+5601	19.67	15.92	$0.019 \pm 0.008$	-	XBL
RXS J1410.5+6100	20.97	14.44	$0.040 \pm 0.011$	-	XBL
2E 1415+2557	19.24	17.54	$0.046 \pm 0.005$	-	XBL
RXS J1456.0+5048	19.94	16.22	$0.082 \pm 0.018$	7.6 <sub>5</sub>	XBL
RXS J1458.4+4832	21.46	18.83	$0.005 \pm 0.002$	-	XBL
1ES 1533+535	19.68	16.72	$0.047 \pm 0.009$	14.6 <sub>5</sub>	XBL
RXS J1756.2+5522	19.90	17.27	$0.043 \pm 0.012$	19.1 <sub>5</sub>	XBL
RXS J2304.6+3705	21.01	17.53	$0.020 \pm 0.003$	9.5 <sub>8</sub>	XBL

## 5. DISCUSSION

The results of our work are consistent with the results of other authors obtained from samples with a significantly smaller number of objects, such as:

- study of the synchrotron component of 300 BL Lac objects in [22] based on non-simultaneous literature data; for the majority of objects,  $\nu_{peak}^s$  is within  $10^{13-14}$  Hz.
- study of the synchrotron component of 105 bright blazars based on the simultaneous measurements of the Planck, Swift, and Fermi telescopes [24], the average  $\nu_{peak}^s$  for FSRQs is  $10^{13.1 \pm 0.1}$  Hz.
- $\nu_{peak}^s$  values estimation using broadband spectral indices  $\alpha_{ro}$  and  $\alpha_{ox}$  (between the frequencies of 5 GHz, 5000 Å and 1 keV) was made in [25, 26]; as a result  $\nu_{peak}^s = 10^{13.02 \pm 0.35}$  Hz for FSRQs and a broad distribution for BL Lacs – from the lowest to the highest frequencies.

In this study most of the objects have  $\nu_{peak}^s 10^{13-14}$  Hz. The HSP blazars are quite rare in the sample – 5% of the total number, these are mostly the BL Lac objects.

The extreme  $\nu_{peak}^s$  values (greater than  $10^{19}$  Hz) were not confirmed for 22 objects from the list of UHBL candidates from [22]. It is easy to notice that in the presence of few points on the SED,  $\nu_{peak}^s$  can often be overestimated, especially if a BL Lac was detected in the high-frequency spectral range. This is true for our sample: all the UHBL candidates are the XBL blazars.

The distributions of  $\nu_{peak}^s$  for FSRQs and BL Lac objects have different characters, which is sometimes interpreted within different morphology of the objects and possible evolution of FSRQs into BL Lac objects [1].

## 6. SUMMARY

We have studied the synchrotron component of the spectral energy distribution (SED) on the sample of 877 blazars of various subclasses. We made an estimation of the synchrotron peak frequency  $\nu_{peak}^s$ , using Roma-BZCAT catalogue and ASCD SED Builder Tool. The following results were obtained:

- The  $\nu_{peak}^s$  values were found for 875 objects. We further classified them by the SED type: 611 (70%) LSPs, 222 (25%) — ISPs and 42 (5%) — HSPs. In the cases of lack of measurements at different wavebands or variable object,  $\nu_{peak}^s$  value estimation is strongly depend on the choice of observational data (active or quiescent state), range of the bands and polynomial degree used for the approximation.
- The distribution of  $\nu_{peak}^s$  peak smoothly decreases towards higher frequencies (Fig. 4). Only 5% of the sample are HSP blazars, most of them are the BL Lacs. It is possible that objects in which electrons are accelerated to very high energies are rare, or it is result of the selection effect
- The distribution of  $\nu_{peak}^s$  is different for FSRQs and BL Lacs. For the BL Lac objects and candidates it is broader and shifted to the more high-frequency region, the average  $\nu_{peak}^s$  value is  $10^{14.6\pm 1.4}$  Hz. For the FSRQs the average  $\nu_{peak}^s$  value is  $10^{13.4\pm 1.0}$  Hz. Statistical tests have shown that  $\nu_{peak}^s$  and flux density  $F_{4.8GHz}$  form different distributions for FSRQs and BL Lacs.
- The  $\nu_{peak}^s$  and  $F_{4.8GHz}$  are also form different distributions for RBL and XBL blazars (at 0.05 confidence level). The average  $\nu_{peak}^s$  is  $10^{13.9\pm 0.9}$  Hz and  $10^{15.9\pm 1.3}$  Hz for RBLs and XBLs, respectively.
- We obtained new estimates of  $\nu_{peak}^s$  for 22 UHBL candidates and found that none of them have  $\nu_{peak}^s > 10^{19}$  Hz. The fact that the majority of measurements were performed in the X-ray band, where they all were detected, was probably the reason of large  $\nu_{peak}^s$  values in [22], where these blazars were classified as Ultra-high energy-peaked. Most of these objects belong to the HSP and partly to the ISP blazars, according to the data collected in the catalogue of Massaro et al.[28].
- We found that 41% of FSRQs and only 9% of BL Lacs in our sample could be considered as candidates to the very low synchrotron peaked blazars (with  $\nu_{peak}^s < 10^{13}$  Hz).

#### ACKNOWLEDGMENTS

The RATAN-600 observations were carried out with the financial support of the Ministry of Education and Science of the Russian Federation and partly with the support of the Russian Foundation for Basic Research (project №12-02-31649). The authors acknowledges support through the Russian Government Program of Competitive Growth of the Kazan Federal University.

We used on-line version of the Roma-BZCAT catalogue and the SED Builder Tool at the ASI Science Data Center (ASDC) website, therefore we are grateful to the ASDC staff. This research has made use of the NASA/IPAC Extragalactic Database (NED) which is operated by the Jet Propulsion Laboratory, California Institute of Technology, under contract with the National Aeronautics and Space Administration.

- 
1. C. M. Urry and P. Padovani, *Publ. Astron. Soc. Pacific* **107**, 803 (1995).
  2. R. M. Sambruna, L. Maraschi, and C. M. Urry, *Astrophys. J.* **463**, 444 (1996).
  3. J. N. Bregman, A. E. Glassgold, P. J. Huggins, et al., *Nature (London)* **293**, 714 (1981).
  4. C. M. Urry and R. F. Mushotzky, *Astrophys. J.* **253**, 38 (1982).
  5. C. D. Impey and G. Neugebauer, *Astron. J.* **95**, 307 (1988).
  6. A. P. Marscher, in *IAU Colloq. 164: Radio Emission from Galactic and Extragalactic Compact Sources*, Edited by J. A. Zensus, G. B. Taylor, and J. M. Wrobel (1998), *Astronomical Society of the Pacific Conference Series*, vol. 144, p. 25.
  7. M. Stickel, P. Padovani, C. M. Urry, et al., *Astrophys. J.* **374**, 431 (1991).
  8. M. Stickel and H. Kuehr, *Astron. and Astrophys. Suppl.* **103**, 349 (1994).
  9. H. Kuehr and G. D. Schmidt, *Astron. J.* **99**, 1 (1990).
  10. T. Maccacaro, I. M. Gioia, D. Maccagni, and J. T. Stocke, *Astrophys. J.* **284**, L23 (1984).
  11. I. M. Gioia, T. Maccacaro, R. E. Schild, et al., *Astrophys. J. Suppl.* **72**, 567 (1990).
  12. J. T. Stocke, J. Liebert, G. Schmidt, et al., *Astrophys. J.* **298**, 619 (1985).
  13. E. S. Perlman, J. T. Stocke, J. F. Schachter, et al., *Astrophys. J. Suppl.* **104**, 251 (1996).
  14. P. Giommi, S. G. Ansari, and A. Micol, *Astron. and Astrophys. Suppl.* **109**, 267 (1995).
  15. P. Giommi and P. Padovani, *Monthly Notices Royal Astron. Soc.* **268**, L51 (1994).
  16. R. E. Wurtz, Ph.D. thesis, UNIVERSITY OF COLORADO AT BOULDER. (1994).
  17. B. Z. Kapanadze, *Astron. J.* **145**, 31 (2013).

18. S. Cutini, S. Ciprini, M. Orienti, et al., *Monthly Notices Royal Astron. Soc.* **445**, 4316 (2014).
19. F. D'Ammando, C. M. Raiteri, M. Villata, et al., *Astron. and Astrophys.* **529**, A145 (2011).
20. P. Giommi, P. Padovani, G. Polenta, et al., *Monthly Notices Royal Astron. Soc.* **420**, 2899 (2012).
21. P. Giommi, P. Padovani, and G. Polenta, *Monthly Notices Royal Astron. Soc.* **431**, 1914 (2013).
22. E. Nieppola, M. Tornikoski, and E. Valtaoja, *Astron. and Astrophys.* **445**, 441 (2006).
23. E. Nieppola, E. Valtaoja, M. Tornikoski, et al., *Astron. and Astrophys.* **488**, 867 (2008).
24. P. Giommi, G. Polenta, A. Lähteenmäki, et al., *Astron. and Astrophys.* **541**, A160 (2012).
25. A. A. Abdo, M. Ackermann, I. Agudo, et al., *Astrophys. J.* **716**, 30 (2010).
26. M. Ackermann, M. Ajello, A. Allafort, et al., *Astrophys. J.* **743**, 171 (2011).
27. E. T. Meyer, G. Fossati, M. Georganopoulos, and M. L. Lister, *Astrophys. J.* **740**, 98 (2011).
28. E. Massaro, P. Giommi, C. Leto, et al., *Astron. and Astrophys.* **495**, 691 (2009).
29. M. G. Mingaliev, Y. V. Sotnikova, R. Y. Udovitskiy, et al., *Astron. and Astrophys.* **572**, A59 (2014).
30. M. G. Mingaliev, Y. V. Sotnikova, I. Tornainen, et al., *Astron. and Astrophys.* **544**, 1 (2012).
31. G. Stratta, M. Capalbi, P. Giommi, et al., *ArXiv e-prints* (2011).
32. S. Antón and I. W. A. Browne, *Monthly Notices Royal Astron. Soc.* **356**, 225 (2005).
33. A. Maselli, E. Massaro, R. Nesci, et al., *Astron. and Astrophys.* **512**, A74 (2010).
34. G. Ghisellini, A. A. Celotti, G. Fossati, et al., *Monthly Notices Royal Astron. Soc.* **301**, 451 (1998).